

1 **THEORY OF (ANTIMICROBIAL) RELATIVITY:**
2 **WHEN COMPETITORS DETERMINE A SPECIES' DRUG SENSITIVITY.**

3 CARLOS REDING^{1*}

4 ¹*Department of Genetics, School of Medicine, Stanford University. Stanford, CA 94304.*

5 *Corresponding author: reding@stanford.edu

6 **Are 'evolution-proof' therapies possible? The use of antimicrobials without imposing selection for**
7 **resistance is conjectured (1, 2) to stop the rise of multi-drug resistance. Here, I present a theory,**
8 **validated experimentally, suggesting a strategy to manipulate antimicrobial sensitivity and achieve**
9 **sustained drug efficacy. The model predicts that accessory microbial species act as drug or carbon**
10 **sink depending on their drug sensitivity, leading to increased drug tolerance or sensitivity in a focal**
11 **species. Aided by this theory, I doubled the sensitivity of *Escherichia coli* MC4100 to tetracycline in**
12 **24h sensitivity tests. The effect was maintained for 168h following serial passages akin to those used**
13 **in evolutionary biology to study antibiotic adaptation in MC4100 (3). This theory, and particularly**
14 **the experimental data, suggest that evolution-proof strategies do exist. My theory can provides**
15 **a framework to design synthetic accessory species that maximise drug efficacy while minimising**
16 **selection on resistance—opening a new venue to treat bacterial infections and, possibly, cancers.**

17 **I. INTRODUCTION**

18 Drug development and therapy design rely on cultures that have only one microbial species, isolated
19 and purified (*pure culture*) (4–7). But the same species is surrounded by many others in nature (8).
20 Such polymicrobial conditions cause changes in drug sensitivity both in microbial pathogens (9–11) and
21 cancers (12, 13), albeit the underlying mechanism is still unknown. The potential of such interactions
22 are clear: Manipulations of polymicrobial environments (i.e. gut microbiota) are used successfully
23 in the clinic to prevent, for example, recurrence of *Clostridium difficile* infections (14). So here I ask
24 the following: Can we combine chemotherapies with *ideal* microbial companions to maximise drug
25 efficacy and reduce selection for resistance?

26 **II. RESULTS**

27 **Drug sensitivity of a focal species is determined by susceptibility of its neighbouring species.** Con-
28 sider j phenotypically distinct species competing for a limited resource, C , and exposed to a drug, A ,
29 cast as the following model:

30
$$\dot{S}_j = \overbrace{G_j(C)S_j}^{\text{Growth}} \cdot \overbrace{I_j(A)}^{\text{Inhibition}}, \quad (1a)$$

31
$$\dot{A}_j = \overbrace{-dA_j}^{\text{Decay}} + \overbrace{\varphi_j(A_e - A_j)S_j}_{\text{Fick's Diffusion}}, \quad (1b)$$

32
$$\dot{A}_e = -dA_e - \sum_{j=1}^i \varphi_j(A_e - A_j)S_j \quad (1c)$$

$$\dot{C} = -\sum_{j=1}^i \overbrace{U_j(C)S_j}^{\text{C-Uptake}} \quad (1d)$$

37

38 Here, \dot{S}_j and \dot{A}_j represent the density of individuals per unit volume from species j and their content of
39 drug A over time, respectively. $U_j(C)$, the uptake rate of resource C —supplied at concentration C_0 —of
40 individuals from species j , is a saturating Monod function proportional to the maximal uptake rate,

$$U_j(C) := \bar{\mu}_j \frac{C}{K_j + C}, \quad (2)$$

42 where K_j is the half-saturation parameter and the affinity of individuals from species j for the limited
43 resource C is given by $1/K_j$. Their growth rate (i.e. absolute fitness) at a given resource concentration
44 is denoted by $G_j(C) := U_j(C) \cdot y_j$, where y_j is the biomass yield per unit of resource in individuals from
45 species j . Their growth inhibition, by drug A , is described qualitatively by the inhibition function (15)

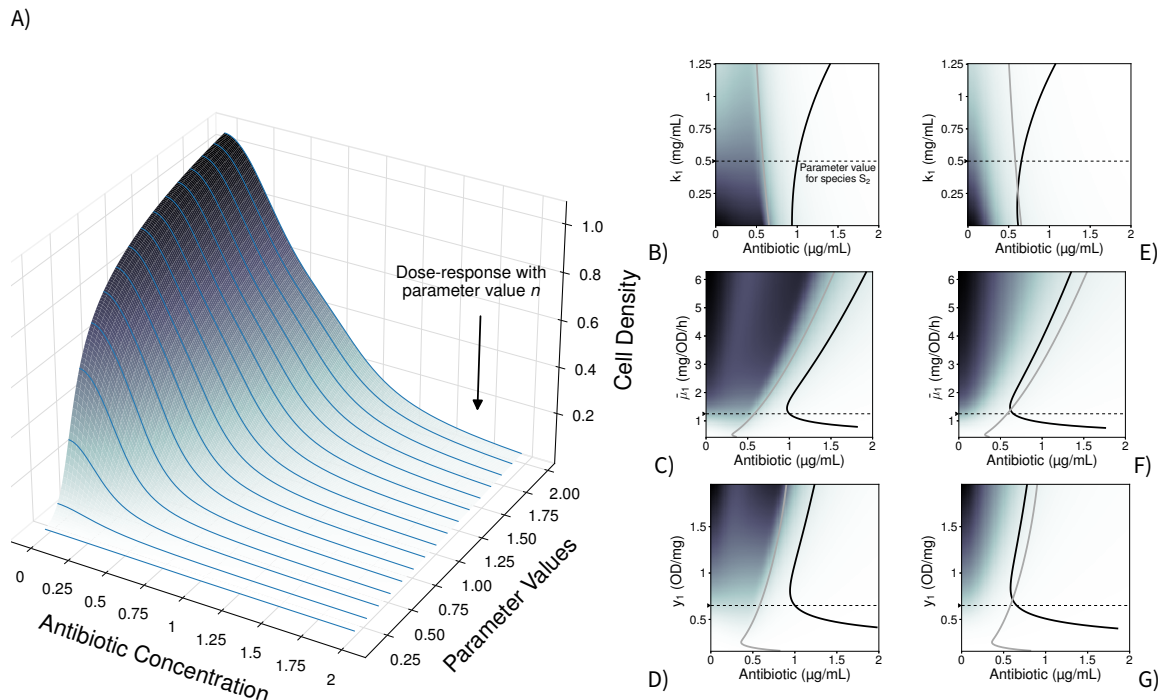
$$I_j(A) := \frac{1}{1 + (A_j/\kappa_j)^\alpha}, \quad \text{where } 0 \leq I_j(A) \leq 1. \quad (3)$$

47 This function is dimensionless and has two parameters. First, the Hill coefficient α which characterises
48 the cooperativity of the inhibition. And second, κ_j is the affinity of drug A for its target and it can be
49 derived from the drug concentration required to halve the maximal growth rate, so that $A_{50} = 1/\kappa_j$
50 (15). Drug A is supplied at concentration A_0 , outside any individuals, at $t = 0$ (so, $A_e(0) = A_0$). The
51 drug then diffuses into individuals from species j with a diffusion coefficient noted by φ_j , and part of
52 A is lost to chemical stability (16) at a rate d .

62 For my first computation I set the number of species $j = 2$, to facilitate later experimental vali-
63 dation, where $I_1(A) = I_2(A)$ and $G_1(C) = G_2(C)$. Thus, individuals from both species are sensitive
64 to A and phenotypically identical. Given Equation 3, the density of individuals from either species as
65 pure cultures declines with higher drug concentrations consistently with standard clinical protocols
66 (5, 7) (Figure 1A). To allow experimental validation, I calculated the concentration of A inhibiting the
67 growth of the pure cultures by 90% (IC_{90}) as commonly used in clinic laboratories (17–19). The drug
68 sensitivity of each species depends on the values for the parameters K , $\bar{\mu}$, and y of Equation 2 (Figure
69 1B–D, grey), with values that increase the density of individuals resulting in higher IC_{90} . This is con-
70 sistent with the *inoculum effect* (20), whereby sensitivity tests using larger inocula also report higher
71 minimum inhibitory concentrations.

72 This phenomenon is exacerbated if both species grow in mixed culture conditions, where both
73 become phenotypically more tolerant to drug A (Figure 1B–D, black). If I were to target, say, individuals
74 from species S_1 , doing so when the species is surrounded by S_2 would require more drug. This is the
75 case of pancreatic ductal adenocarcinoma with bacteria growing in its microenvironment (12). More
76 generally, genotypes analog to S_1 should increase their drug tolerance when they are surrounded by
77 similarly sensitive species.

78 To test this hypothesis, I mixed equal proportions of *Escherichia coli* Wyl and *Salmonella typhimurium*
79 SL1344 in minimal media supplemented with different concentrations of tetracycline (see Methods).
80 Both species have similar sensitivity to this antibiotic, 0.232 ± 0.003 and 0.276 ± 0.016 $\mu\text{g/mL}$ of tetra-
81 cycline (mean $IC_{90} \pm 95\%$ confidence, with $n = 8$ replicates, see Methods). This approximates to

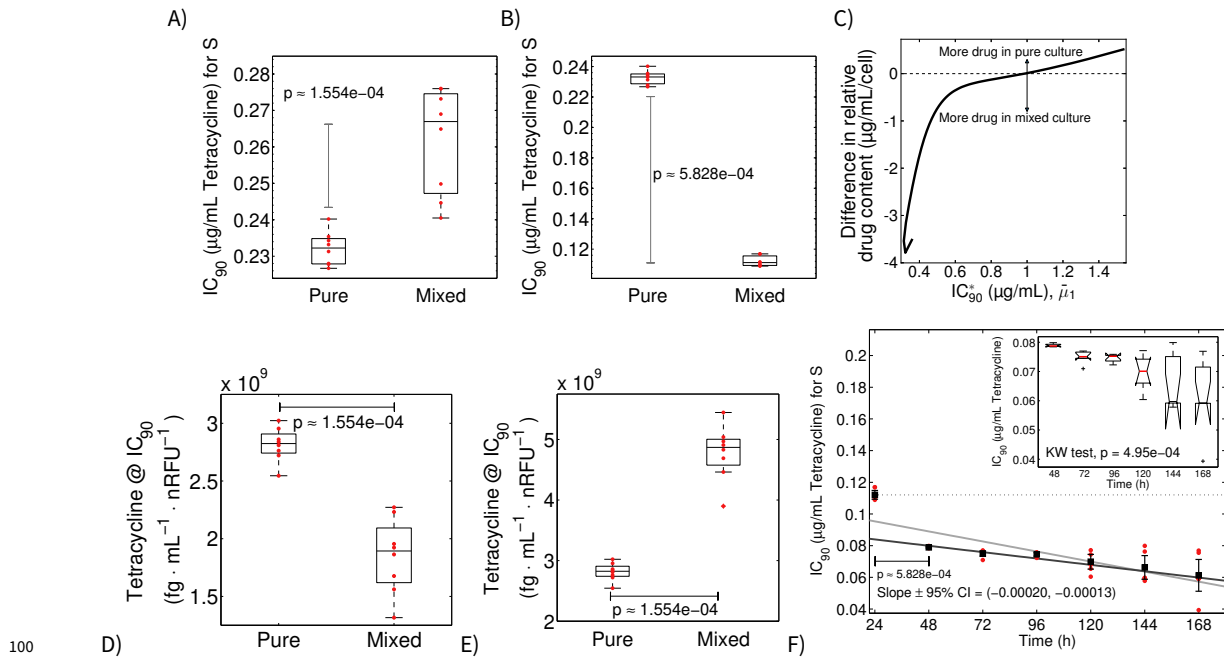


53 **Figure 1. S_1 drug sensitivity profiles in pure and mixed culture growth conditions alongside accessory species S_2 .** A) Growth of species S_1 , with different parameter values (k_1 , $\bar{\mu}_1$, and y_1), after 24h of growth in the presence of different antibiotic concentrations. I aggregated the resulting dose-response profiles (blue) to create a density map from low predicted cell density (white) to high predicted cell density (black). B–D) IC₉₀, antibiotic concentration inhibiting 90% (IC₉₀) the growth predicted without drug, resulting with different parameters values for k_1 (B), $\bar{\mu}_1$ (C), or y_1 (D) in equation 1 when species S_2 is drug-sensitive. The IC₉₀ for species S_1 growing as pure cultures is shown in grey, and growing in mixed culture with S_2 are shown in black. The parameter values for species S_2 were fixed at a value noted by a black arrow on the y-axis, followed by a dotted black line. E–G) Change in IC₉₀, as in Figures B–C), when the competing species S_2 is not drug-sensitive.

82 $I_1(A) \approx I_2(A)$, as laid out by the theory above. The chromosome of *E. coli* Wyl carries *yfp*, gene encoding a yellow fluorescence protein (YFP), so I tracked its density in mixed culture conditions. Consistently with Equations 1a–d, the bacterium was around 23% more tolerant to tetracycline when it grew in mixed culture with *S. typhimurium* (Mann-Whitney U-test $p = 1.554 \times 10^{-4}$, $ranksum = 36$ with $n = 8$ replicates, Figure 2A).

87 Next, I explored in the model the case where individuals from both species have different sensitivities to drug A ($I_1(A) \neq I_2(A)$). This scenario is akin to pathogens such as *C. difficile* growing alongside human cells (14) where the latter are unaffected by the drug ($I_2(A) \approx 1$). The model now predicts a subset of values for K , y , and $\bar{\mu}$ that make S_1 more sensitive to the drug in the presence of individuals from species S_2 (Figure 1E–G). To test this prediction, I mixed equal proportions of two constructs of *Escherichia coli* with different sensitivities to tetracycline. One construct is Wyl, used above, who is sensitive to the antibiotic. The other construct is GB(c), harbouring a non-transmissible plasmid carrying the gene *tet(36)* (21) and, therefore, resistant to the drug. Tetracycline binds to the bacterial ribosome, inhibiting protein synthesis (22), and *tet(36)* provides ribosomal protection against tetracycline (21) without degrading the antibiotic. The IC₉₀ for this construct was 6.106 ± 0.272 µg/mL of tetracycline (mean IC₉₀ \pm 90% confidence with $n = 8$ replicates). Now, $I_2(A) \ll I_1(A)$ satisfies the assumption above. The IC₉₀ for *E. coli* Wyl was 0.232 ± 0.003 µg/mL of tetracycline as pure culture.

99 Growing alongside drug-resistant GB(c), however, it was $0.112 \pm 0.003 \mu\text{g/mL}$ (Figure 2B).



101 **Figure 2. Changes in IC_{90} of drug-sensitive *Escherichia coli* Wyl are consistent with theoretical predictions. A–B)** IC_{90}
 102 for tetracycline of *Escherichia coli* Wyl in pure culture, and in mixed culture with *Salmonella typhimurium* (A) and *Escherichia*
 103 *coli* GB(c) (B). The IC_{90} for *S. typhimurium* in pure culture was $0.276 \pm 0.016 \mu\text{g/mL}$ of tetracycline (mean \pm 95% confidence),
 104 and $6.106 \pm 0.272 \mu\text{g/mL}$ for *E. coli* GB(c). The box plot shows the median (centre of the box), 25th, and 75th percentile of
 105 the dataset. The whiskers extend to the most extreme data points that are not outliers, which are individually represented.
 106 Raw data is represented as red dots. The p value shown corresponds to a Mann-Whitney U-test. **C)** Theoretical difference
 107 in relative drug content—antibiotic molecules per cell—of S_1 between pure culture conditions, and mixed culture with *drug-*
 108 *sensitive* S_2 for different $\bar{\mu}_1$ values (for all parameters in Figure S1). Positive values denote higher content of antibiotic per
 109 cell in pure culture conditions, whereas negative values denote higher antibiotic per cell in mixed culture. Lack of difference
 110 is represented by a horizontal, dotted line. **D–E)** Estimation of tetracycline content from experimental data of *E. coli* Wyl
 111 growing alongside *Salmonella typhimurium* (D) and *E. coli* GB(c) (E). The box plots show the median (centre of the box),
 112 25th, and 75th percentile of the dataset. The whiskers extend to the most extreme data points that are not outliers, which
 113 are individually represented. Raw data is represented as red dots. The p value shown corresponds to a Mann-Whitney U-
 114 test. **F)** Variation in IC_{90} of *E. coli* Wyl in mixed culture over time. The errorbars denote mean IC_{90} and 95% confidence,
 115 and raw data is shown as red dots. The p value shown corresponds to a Mann-Whitney U-test. I fitted a linear model to IC_{90} data
 116 including (grey) and excluding the IC_{90} at 24h, and showed the slope parameter of the case with the lowest p . The inset
 117 show the p value of a Kruskal Wallis one-way ANOVA applied to IC_{90} data excluding that measured at 24h. The box plot
 118 shows the median in red, 25th, and 75th percentile of the dataset. The whiskers extend to the most extreme data points
 119 that are not outliers, which are individually represented as a black cross.

121 **Neighbouring species S_2 determines drug availability for S_1 .** Above I noted that parameter values
 122 leading to higher density of individuals in pure culture, also led to higher IC_{90} . When $I_1(A) \approx I_2(A)$,
 123 Equations 1a–d suggest that individuals from one species change the drug availability, measured as rel-
 124 ative drug molecules per individual, for the other. Thus, when species S_2 absorbs its share of drug in
 125 mixed culture conditions, there is less of it available for species S_1 resulting in less drug per individual
 126 (Figure S1A–C)—and *vice versa*. However, when $I_1(A) \neq I_2(A)$, the least sensitive species barely ab-
 127 sorbs drug. The change in drug availability occurs through a different mechanism. The least sensitive

128 species is able to remove a higher share of the limited resource, C , as its growth is unaffected by the
129 drug. Thus, the growth of the most sensitive species is limited (23), leaving more drug per individual
130 of this species (Figure S1D–F).

131 To verify this rationale, I estimated the content of tetracycline in *E. coli* Wyl by dividing the bac-
132 terium's culture density, measured in relative fluorescence units to allow tracking in mixed culture
133 conditions, by the concentration of tetracycline defining its IC_{90} . The estimates resemble closely the
134 theoretical predictions in Figure 2C: *E. coli* Wyl contains approximately 20% less tetracycline grow-
135 ing next to *Salmonella typhimurium* (Figure 2D) and 65% more tetracycline growing alongside drug-
136 resistant GB(c) (Figures 2E).

137 Now, experiments of parallel evolution show that *acr*, operon responsible for the multi-drug efflux
138 pump AcrAB-TolC (24), undergoes genomic amplification in *E. coli* MC4100 (3). Thus, MC4100 over-
139 comes the exposure to doxycycline, a type of tetracycline drug, within five days given its increased
140 capacity to remove antibiotic molecules (3). Other strains of *E. coli* show identical adaptation (25). To
141 test whether Wyl, MC4100 derivative sensitive to tetracycline, overcomes its exposure to the drug I
142 propagated a culture containing equal proportions of *E. coli* Wyl and GB(c) for 168h. If Wyl acquires a
143 mutation, such as the amplification of *acr*, that protects it against tetracycline I would expect greater
144 IC_{90} over time. However, as Figure 2F illustrates, the IC_{90} of Wyl was further reduced during this
145 period.

146 III. DISCUSSION

147 My theory reconciles the unexpected observations found in direct sensitivity tests (5, 9, 26)—drug sen-
148 sitivity tests that skip isolation and purification of the pathogenic agent (27–29). Using direct testing,
149 pathogens known to be sensitive to a drug can be interpreted as resistant and *vice versa* (9, 30). While
150 direct testing shortens turnaround time in hospitals, allowing to initiate therapies earlier (31), interna-
151 tional guidelines (5) do not recommended as they can be misleading. A simple mathematical model
152 can explain why such inconsistencies occur.

153 ‘Evolution-proof’ therapies are the next frontier in the treatment of infectious diseases (2) and can-
154 cers (32), but their existence is still a conjecture. The above inconsistencies highlight that pathogens
155 can have multiple sensitivities to the same drug, and they are predictable so they can be used to de-
156 velop strategies that ‘sensitise’ cancers and pathogens to chemotherapies. Mine is a very simple model
157 inspired by the polymicrobial ecosystem where pathogens thrive, and I do not wish to over state its pre-
158 dictive power. For example, it lacks an immune response or environmental complexities found in the
159 human body. But it shows that evolution-proof strategies are indeed possible. The increased disper-
160 sion of my evolutionary dataset after 168h suggests adaptation of Wyl. However, its sensitivity still
161 remained high, as given by its IC_{90} .

162 This work is focused on bacteria because they can easily be grown in a laboratory or labelled. But
163 the model can also apply to cancers. They, too, can have different sensitivities to chemotherapies
164 depending on the bacteria growing in their microenvironment (12, 13). Interestingly, the drug content
165 in pancreatic ductal adenocarcinoma is lower when bacteria are present (12). My model suggests these
166 bacteria would be absorbing part of the drug.

167 IV. METHODS

168 **Media and Strains.** The strains of *Escherichia coli* GB(c) and Wyl (33) were a gift from Remy Chait
169 and Roy Kishony, and *Salmonella typhimurium* SL1344 (34) a gift from Markus Arnoldini and Martin
170 Ackermann. Experiments were conducted in M9 minimal media supplemented with 0.4% glucose and
171 0.1% casamino acids and supplemented with tetracycline. I made tetracycline stock solutions from
172 powder stock (Duchefa #0150.0025) at 5mg/mL in deionised water. Subsequent dilutions were made
173 from this stock and kept at 4°C.

174 **Sensitivity assay.** I inoculated a 96-well microtitre plate, containing 150µg/mL of media supplemented
175 with 0–0.5 µg/mL of tetracycline (for *E. coli* Wyl and *S. typhimurium*) or 0–15µg/mL (for *E. coli* GB(c)),
176 with an overnight of each strain to measure drug sensitivity in pure cultures. For sensitivity assays of
177 Wyl in mixed culture conditions I inoculated the microtitre plate, containing 150µg/mL of media sup-
178 plemented with 0–0.5 µg/mL of tetracycline, with equal proportions of two overnight cultures: Wyl +
179 GB(c) or Wyl + *S. typhimurium*.

180 I incubated the microtitre plate at 30°C in a commercial spectrophotometer and measured the
181 optical density of each well at 600nm (OD_{600}), yellow fluorescence for the S strain (YFP excitation at
182 505nm, emission at 540nm), and cyan fluorescence for the R strain (CFP at 430nm/480nm) every 20min
183 for 24h. I defined the minimum inhibitory concentration as the tetracycline concentration able to
184 inhibit 90% of the growth observed in the absence of antibiotic after the 24h incubation period.

185 **Culture readings.** Fluorescence protein genes were constitutively expressed with an approximately
186 constant fluorescence to optical density ratio (Figure S2). The number of colony forming units (CFU) is
187 positively correlated with optical density measured at 600nm (OD_{600}) (Figure S3). Thus, I normalised
188 fluorescence readings with respect to optical density readings, using the ratio optical density to flu-
189 orescence that I in pure culture conditions, to track the relative abundance of Wyl in mixed culture
190 conditions.

191 I imported the resulting time series data set into MATLAB R2014b and subtracted the background,
192 from inoculum size at $t = 0$, using the following algorithm. First, I fitted three mathematical models
193 to data: 1) linear model $g(t) = b + f \cdot t$, 2) exponential model $g(t) = b + C \cdot \exp(f \cdot t)$ and 3) logistic
194 model $g(t) = b + K/(1 + C \cdot \exp(-f \cdot t))$. The terms $g(t)$ denote culture growth through time (in OD,
195 YFP, or CFP units), b the inoculum size used to subtract the background, C is a parameter and K the
196 maximal population size attained.

197 **Evolutionary dataset.** Following the protocol in Reference (3) I propagated a mixed culture, growing
198 in a 96-well microtitre plate containing 150µg/mL of media supplemented with 0–0.5 µg/mL of tetracy-
199 cline, into a new microtitre plate containing fresh media and antibiotic every 24h. Growth data was
200 blank corrected as above, and used to calculate the IC_{90} .

201 **Code availability:** A python implementation of equations 1a–d can be found at [https://github.com/rc-](https://github.com/rc-redding/papers/tree/master/EvolProof_2020)
202 [redding/papers/tree/master/EvolProof_2020](https://github.com/rc-redding/papers/tree/master/EvolProof_2020) . The parameter values used can be found in Table S1.

203 **Competing interests:** The author declares no competing interests.

204 **REFERENCES**

- 205 1. Allen, R. C., Popat, R., Diggle, S. P. & Brown, S. P. Targeting virulence: can we make evolution-
206 proof drugs? *Nat. Rev. Microbiol.* **12**, 300–308 (2014).
- 207 2. Bell, G. & MacLean, C. The Search for ‘Evolution-Proof’Antibiotics. *Trends Microbiol.* (2017).
- 208 3. Pena-Miller, R., Laehnemann, D., Jansen, G., *et al.* When the most potent combination of an-
209 tibiotics selects for the greatest bacterial load: the smile-frown transition. *PLoS Biol.* **11**, e1001540
210 (2013).
- 211 4. Russell, B. M., Udomsangpetch, R., Rieckmann, K. H., *et al.* Simple in vitro assay for determining
212 the sensitivity of Plasmodium vivax isolates from fresh human blood to antimalarials in areas
213 where P. vivax is endemic. *Antimicrob. Agents. Chemother.* **47**, 170–173 (2003).
- 214 5. *Performance Standards for Antimicrobial Susceptibility Testing; Twenty-Second Informational Supple-*
215 *ment M100-S22* 3. Clinical and Laboratory Standards Institute (2012). ISBN: 1-56238-786-3.
- 216 6. Bennett, J., Dolin, R. & Blaser, M. *Principles and Practice of Infectious Diseases Churchill Livingstone*
217 **v. 1**. ISBN: 9781455748013 (Elsevier - Health Sciences Division, 2014).
- 218 7. *Antimicrobials susceptibility testing version 5.0* European Committee on Antimicrobial Susceptibil-
219 ity Testing (European Committee on Antimicrobial Susceptibility Testing, Jan. 2015).
- 220 8. Hibbing, M. E., Fuqua, C., Parsek, M. R. & Peterson, S. B. Bacterial competition: surviving and
221 thriving in the microbial jungle. *Nat. Revs. Microbiol.* **8**, 15–25 (2010).
- 222 9. Shahidi, A. & Ellner, P. D. Effect of mixed cultures on antibiotic susceptibility testing. *Appl. Mi-*
223 *crobiol.* **18**, 766–770 (1969).
- 224 10. Lasa, I. & Solano, C. Polymicrobial infections: Do bacteria behave differently depending on their
225 neighbours? *Virulence* **9**, 895–897 (2018).
- 226 11. Galera-Laporta, L. & Garcia-Ojalvo, J. Antithetic population response to antibiotics in a polybac-
227 terial community. *Sci. Adv.* **6**, eaaz5108 (2020).
- 228 12. Geller, L. T., Barzily-Rokni, M., Danino, T., *et al.* Potential role of intratumor bacteria in mediating
229 tumor resistance to the chemotherapeutic drug gemcitabine. *Science* **357**, 1156–1160 (2017).
- 230 13. Sedighi, M., Zahedi Bialvaei, A., Hamblin, M. R., *et al.* Therapeutic bacteria to combat cancer;
231 current advances, challenges, and opportunities. *Cancer Med.* **8**, 3167–3181 (2019).
- 232 14. Burke, K. E. & Lamont, J. T. Fecal Transplantation for Recurrent Clostridium difficile Infection in
233 Older Adults: A Review. *J. Am. Geriatr. Soc.* **61**, 1394–1398 (2013).
- 234 15. Klumpp, S., Zhang, Z. & Hwa, T. Growth rate-dependent global effects on gene expression in
235 bacteria. *Cell* **139**, 1366–1375 (2009).
- 236 16. Gómez-Pacheco, C., Sánchez-Polo, M, Rivera-Utrilla, J & López-Peñalver, J. Tetracycline degrada-
237 tion in aqueous phase by ultraviolet radiation. *Chem. Eng. J.* **187**, 89–95 (2012).
- 238 17. Cedillo-Rivera, R & Munoz, O. In-vitro susceptibility of Giardia lamblia to albendazole, mebenda-
239 zole and other chemotherapeutic agents. *J. Med. Microbiol.* **37**, 221–224 (1992).

- 240 18. Cottrell, M. L., Hadzic, T. & Kashuba, A. D. Clinical pharmacokinetic, pharmacodynamic and
241 drug-interaction profile of the integrase inhibitor dolutegravir. *Clin. Pharmacokinet.* **52**, 981–994
242 (2013).
- 243 19. Baumgartner, M., Bayer, F., Pfrunder-Cardozo, K. R., Buckling, A. & Hall, A. R. Resident microbial
244 communities inhibit growth and antibiotic-resistance evolution of *Escherichia coli* in human gut
245 microbiome samples. *PLoS Biol.* **18**, e3000465 (2020).
- 246 20. Eng, R., Smith, S. & Cherubin, C. Inoculum effect of new beta-lactam antibiotics on *Pseudomonas*
247 *aeruginosa*. *Antimicrob. Agents. Chemother.* **26**, 42–47 (1984).
- 248 21. Whittle, G., Whitehead, T. R., Hamburger, N., Shoemaker, N. B., Cotta, M. A., *et al.* Identification
249 of a new ribosomal protection type of tetracycline resistance gene, tet(36), from swine manure
250 pits. *Appl. Environ. Microbiol.* **64**, 4151–4158 (2003).
- 251 22. Epe, B & Woolley, P. The binding of 6-demethylchlortetracycline to 70S, 50S and 30S ribosomal
252 particles: a quantitative study by fluorescence anisotropy. *EMBO J.* **3**, 121–126 (1984).
- 253 23. Day, T., Huijben, S. & Read, A. F. Is selection relevant in the evolutionary emergence of drug
254 resistance? *Trends Microbiol.* **23**, 126–133 (2015).
- 255 24. Okusu, H., Ma, D. & Nikaido, H. AcrAB efflux pump plays a major role in the antibiotic resistance
256 phenotype of *Escherichia coli* multiple-antibiotic-resistance (Mar) mutants. *J. Bacteriol.* **178**, 306–
257 308 (1996).
- 258 25. Ayari, Jessica, P., Fabio, G., *et al.* Using a Sequential Regimen to Eliminate Bacteria at Sublethal
259 Antibiotic Dosages. *PLoS Biol.* **13**, e1002104 (Apr. 2015).
- 260 26. Ellner, P. D. & Johnson, E. Unreliability of Direct Antibiotic Susceptibility Testing on Wound Ex-
261 udates. *Antimicrob. Agents. Chemother.* **9**, 355–356 (1976).
- 262 27. Serisier, D. J., Jones, G., Tuck, A., Connett, G. & Carroll, M. P. Clinical application of direct sputum
263 sensitivity testing in a severe infective exacerbation of cystic fibrosis. *Pediatr. Pulmonol.* **35**, 463–
264 466 (2003).
- 265 28. Jabeen, K., Kumar, H., Farooqi, J., *et al.* Agreement of direct antifungal susceptibility testing from
266 positive blood culture bottles with the conventional method for *Candida* species. *J. Clin. Microbiol.*
267 **54**, 343–348 (2016).
- 268 29. Qamar, F. N., Yousafzai, M. T., Khalid, M., *et al.* Outbreak investigation of ceftriaxone-resistant
269 *Salmonella enterica* serotype Typhi and its risk factors among the general population in Hyder-
270 abad, Pakistan: a matched case-control study. *Lancet Infect. Dis.* **18**, 1368–1376 (2018).
- 271 30. Ellis, L. Criminal behavior and r/k selection: An extension of gene-based evolutionary theory.
272 *Deviant Behav* **8**, 149–176 (1987).
- 273 31. Coorevits, L., Boelens, J. & Claeys, G. Direct susceptibility testing by disk diffusion on clinical
274 samples: a rapid and accurate tool for antibiotic stewardship. *Eur. J. Clin. Microbiol. Infect. Dis.* **34**,
275 1207–1212 (2015).
- 276 32. Archetti, M. & Pienta, K. J. Cooperation among cancer cells: applying game theory to cancer. *Nat.*
277 *Rev. Cancer* **19**, 110–117 (2019).

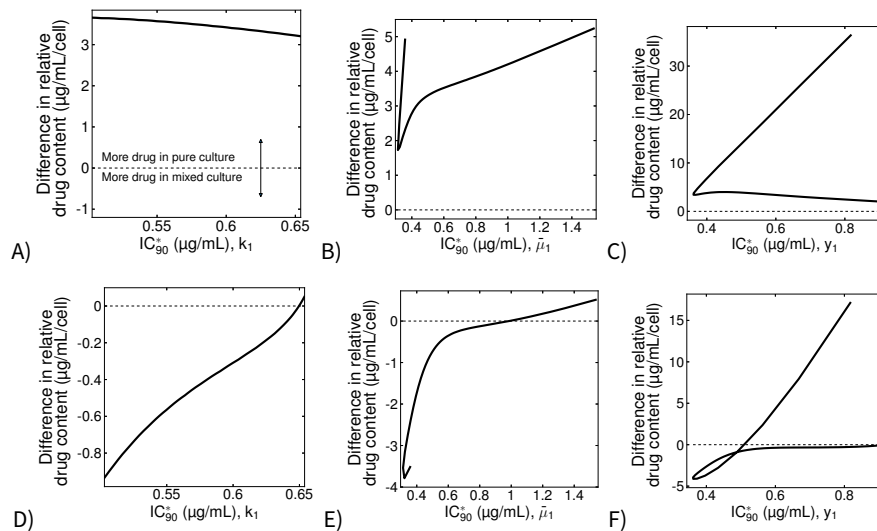
- 278 33. Chait, R., Craney, A & Kishony, R. Antibiotic interactions that select against resistance. *Nature*
279 **446**, 668–671 (2007).
- 280 34. Arnoldini, M., Vizcarra, I. A., Peña-Miller, R., *et al.* Bistable expression of virulence genes in
281 salmonella leads to the formation of an antibiotic-tolerant subpopulation. *PLoS Biol.* **12**, e1001928
282 (2014).

283 **V. SUPPLEMENTARY TABLES**

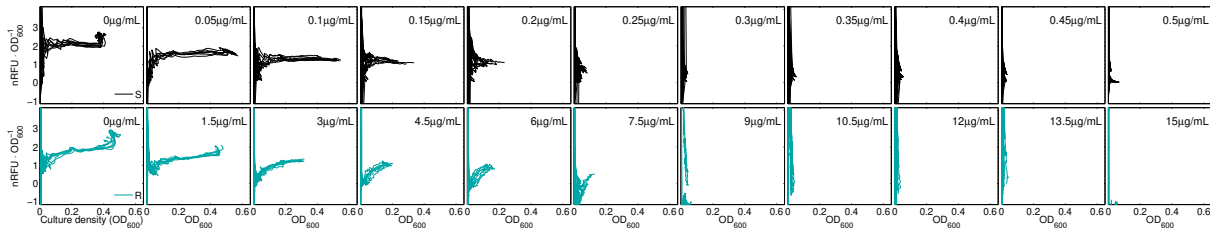
Table S1. Model parameters for Equations 1a–d, 2 and 3.

Parameter	Description	Value
$\bar{\mu}_j$	Maximal carbon uptake rate	1.25 mg / OD / h
K_j	Half-saturation constant	0.5 mg / mL
y_j	Biomass yield	0.65 OD / mg
d	Drug degradation rate	10^{-4} / h
κ_j	Affinity of drug A for species type j	0.1 mL / μ g
φ_j	Diffusion coefficient	0.1 mm ² / s
A_0	Initial drug concentration	2 μ g / mL
C_0	Initial carbon concentration	2 mg / mL

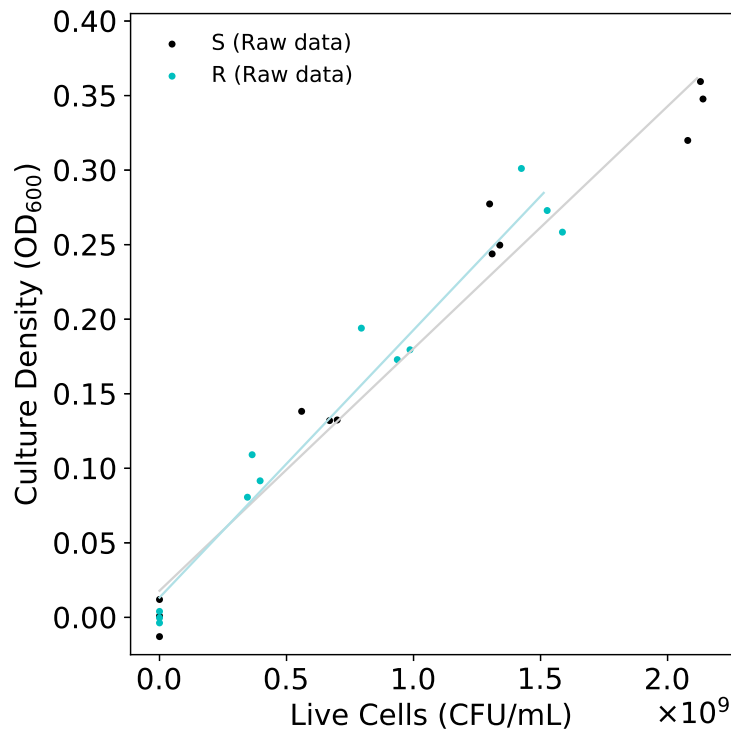
284 **VI. SUPPLEMENTARY FIGURES**



285 **Figure S1. Drug concentration in individuals from species S_1 in pure and mixed growth conditions.** A–C) Theoretical dif-
 286 ference in relative drug content—antibiotic molecules per cell—of S_1 between pure culture conditions, and mixed culture
 287 with *drug-sensitive* S_2 . A), B) and C) illustrate the prediction when changing the parameter k , $\bar{\mu}$, and y , respectively. The
 288 difference is positive (>0) when the relative content of antibiotic is higher in pure culture conditions, whereas is negative
 289 (<0) when the content is higher in mixed culture conditions. Lack of difference is represented by a horizontal, dotted line.
 290 **D–F)** Theoretical difference in relative drug content—antibiotic molecules per cell—of S_1 between pure culture conditions,
 291 and mixed culture with *drug-insensitive* S_2 . A), B) and C) illustrate the prediction when changing the parameter k , $\bar{\mu}$, and
 292 y , respectively. The difference is positive (>0) when the relative content of antibiotic is higher in pure culture conditions,
 293 whereas is negative (<0) when the content is higher in mixed culture conditions. Lack of difference is represented by a hori-
 294 zontal, dotted line.



296 **Figure S2. Changes in relative fluorescence over time in both Wyl and GB(c) strains.** Raw change in fluorescence, per
297 optical density units, measured every 20min for 24h for *E. coli* Wyl (black) and GB(c). Each column represents the data set
298 for each tetracycline concentration used.



300 **Figure S3. Calibration curve to translate optical density data to number of *Escherichia coli* cells.** I fitted the linear
301 model $a = bx + c$ to optical density and colony counting data (dots) to calculate the number of optical density units
302 (OD_{600}) per cell. a denotes the optical density readings measured at 600nm, c the crossing point with the y -axis when
303 $x = 0$, and b the conversion factor between optical density and number of cells (x). I interpolating optical density readings
304 to calculate the number of cells within a culture as $x = (a - c)/b$. For the strain S, $b = 1.62 \times 10^{-10} OD \cdot mL \cdot CFU^{-1}$
305 and $c = 1.78 \times 10^{-2} OD$, whereas for R $b = 1.79 \times 10^{-10} OD \cdot mL \cdot CFU^{-1}$ and $c = 1.33 \times 10^{-2} OD$.